

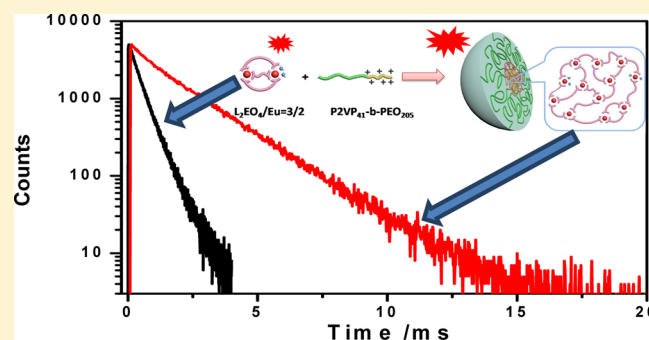
Understanding the Structure of Reversible Coordination Polymers Based on Europium in Electrostatic Assemblies Using Time-Resolved Luminescence

Limin Xu, Mengqi Xie, Jianbin Huang,* and Yun Yan*

Beijing National Laboratory for Molecular Sciences (BNLMS), State Key Laboratory for Structural Chemistry of Unstable and Stable Species, College of Chemistry and Molecular Engineering, Peking University, Beijing 100871, China

Supporting Information

ABSTRACT: In situ characterization of the structure of reversible coordination polymers remains a challenge because of their dynamic and concentration-responsive nature. It is especially difficult to determine these structures in their self-assemblies where their degree of polymerization responds to the local concentration. In this paper, we report on the structure of reversible lanthanide coordination polymers in electrostatic assemblies using time-resolved luminescence (TRL) measurement. The reversible coordinating system is composed of the bifunctional ligand 1,11-bis(2,6-dicarboxypyridin-4-yloxy)-3,6,9-trioxaundecane (L_2EO_4) and europium ion Eu^{3+} . Upon mixing with the positively charged diblock copolymer poly(2-vinylpyridine)-*b*-poly(ethylene oxide) ($P2VP_{41}$ -*b*- PEO_{205}), electrostatic polyion micelles are formed and the negatively charged L_2EO_4 -Eu coordination complex simultaneously transforms into coordination “polymers” in the micellar core. By virtue of the water-sensitive luminescence of Eu^{3+} , we are able to obtain the structural information of the L_2EO_4 -Eu coordination polymers before and after the formation of polyion micelles. Upon analyzing the fluorescence decay curves of Eu^{3+} before and after micellization, the fraction of Eu^{3+} fully coordinated with L_2EO_4 is found to increase from 32 to 83%, which verifies the occurrence of chain extension of the L_2EO_4 -Eu coordination polymers in the micellar core. Our work provides a qualitative picture for the structure change of reversible coordination polymers, which allows us to look into these “invisible” structures.



INTRODUCTION

Recently, reversible coordination polymers have emerged as a novel kind of building blocks for supramolecular self-assemblies owing to their structural and compositional advantages.^{1–10} These are equilibrium supramolecular structures with alternatively appearing ligands and metal ions.^{1–10} The coordination centers usually carry charges that allow these untraditional polyelectrolytes to interact with oppositely charged species just like their conventional counterparts.^{11–16} However, theoretical calculations predict that they respond quickly to changes in the concentration and composition owing to the dynamic formation and breakup of the coordinating bonds.¹⁷ This makes it exceedingly difficult to experimentally characterize these macromolecular structures,¹⁸ and so far, little in situ structural information is available for this type of material.^{18,19} The situation becomes even more complicated when the coordination complexes form self-assemblies via electrostatic interactions.^{20–24} The local concentration of the coordination complexes may increase in the presence of an oppositely charged polyelectrolyte, which spontaneously leads to a chain growth of the coordination complexes owing to their concentration responsiveness. This means that one may expect a different structure for the coordination complexes before and

after the electrostatic self-assembly formation. We have reported several typical examples of the electrostatic assembly of coordination polymers in previous works,^{20,21,25–27} from where we infer that the coordination oligomers may grow into polymers owing to the enhancement of their local concentration in the presence of an oppositely charged polyelectrolyte. However, until then, we do not have qualitative proof for such a chain extension because direct measurement of the degree of polymerization and the mass of a single chain is impossible in the electrostatic assemblies.

In the present study, we utilize time-resolved europium luminescence to obtain the information of chain extension of coordination polymers based on europium in electrostatic assemblies. It is well known that the luminescence of europium is very sensitive to water molecules bonded in the first coordination sphere.^{28–30} In an aqueous solution, the Eu^{3+} ions show very weak luminescence because of the formation of $Eu(H_2O)_8^{3+}$ and $Eu(H_2O)_9^{3+}$ complexes, which is in an equilibrium owing to the maximum coordinating number of 9

Received: March 13, 2016

Revised: May 19, 2016

Published: May 26, 2016

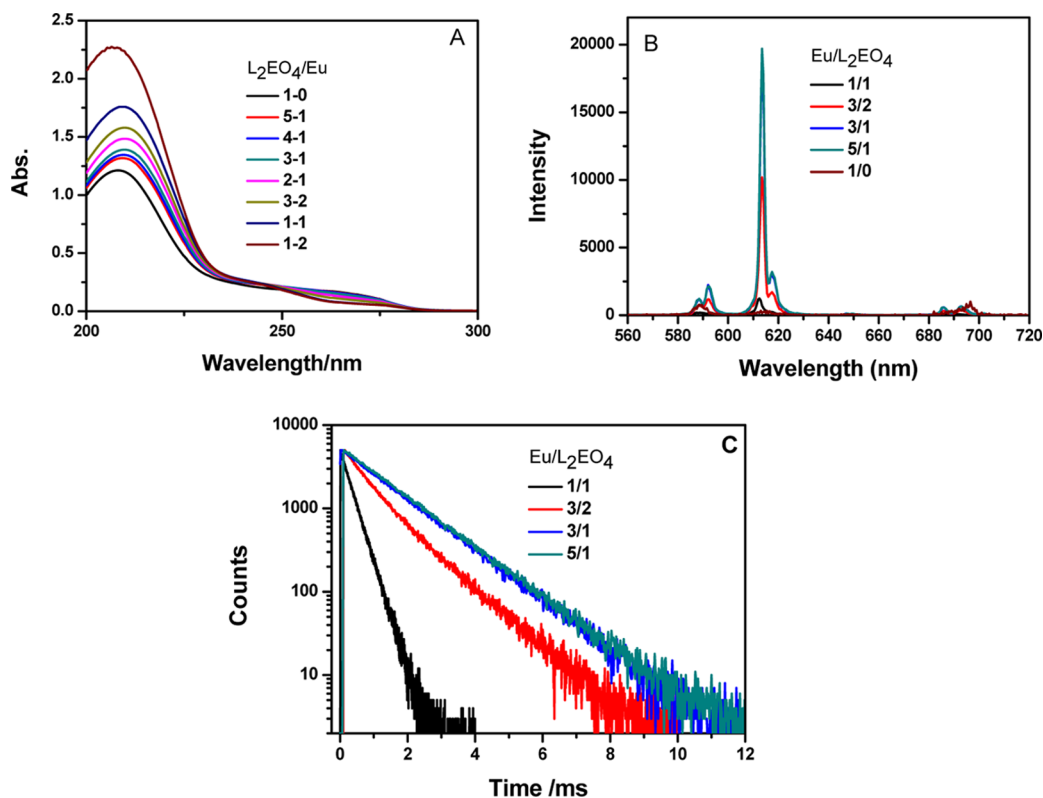


Figure 1. (A) UV-vis absorption spectra, (B) emission spectra, and (C) TRL spectra of L_2EO_4/Eu complexes at various molar ratios. The concentration of L_2EO_4 is fixed at 0.02 mM ($[L_2EO_4] = 0.02$ mM) in (A) and that of Eu^{3+} varies with the change in the molar ratio; however, in (B, C), the excitation is fixed at 395 nm ($\lambda_{ex} = 395$ nm), $[Eu^{3+}] = 0.67$ mM, pH = 6.9.

for the Eu^{3+} . However, by replacing water molecules with proper ligands, the luminescence of europium can be enhanced significantly.^{25,31–36} We have shown that in case the coordination supramolecular polymers are constructed with europium and 1,11-bis(2,6-dicarboxypyridin-4-yloxy)-3,6,9-trioxaundecane (L_2EO_4), the luminescence of europium can be greatly enhanced.²⁵ Upon combining the coordination complexes and the block copolymer $PMVP_{41}$ - PEO_{205} , the luminescence can be further enhanced, which is attributed to the chain extension triggered by the enhanced local concentration of the coordination polymers in the electrostatic assemblies. We have reported the static luminescence enhancement effect of L_2EO_4 - Eu in the electrostatic micelles.²⁵ Here, we show that upon application of time-resolved luminescence (TRL), we are able to infer the most possible structure of the L_2EO_4 - Eu complex in a dilute solution. Also, we verified the growth of the chain length of the L_2EO_4 - Eu complex in the electrostatic micelles. Our work provides a simple way to probe the in situ structure of dynamic coordination supramolecules, which helps to understand and estimate their behavior and contribution in various applications.

EXPERIMENTAL SECTION

Materials. The bisligand L_2EO_4 used in this work was prepared according to previously reported procedures.^{20,37} A diblock polymer, poly(2-vinylpyridine)-*b*-poly(ethylene oxide) ($P2VP_{41}$ -*b*- PEO_{205} , $M_w = 13.3$ k, PDI = 1.05), was obtained from Polymer Source. $Eu(NO_3)_3 \cdot 6H_2O$ (99.99%) was obtained from Sigma. Stock solutions of $P2VP_{41}$ -*b*- PEO_{205} , L_2EO_4 , and $Eu(NO_3)_3$ were prepared at appropriate concentrations. To prepare the Eu coordination complexes, 20 mM L_2EO_4 solution and 50 mM $Eu(NO_3)_3$ solution were mixed at the desired molar ratios. The coordination complexes were added in

stoichiometric amounts to a $P2VP_{41}$ -*b*- PEO_{205} aqueous solution ($[P2VP] = 2$ mM, $[L_2EO_4] = 1$ mM, and $[Eu^{3+}] = 0.67$ mM). HCl and KOH were used to control the pH instead of buffer to avoid the possible coordination between the buffering components and the europium ion. Ultrapure water was used, and no extra salt was added.

Methods. Luminescence Measurements. A steady-state spectrometer FLS920 was used to measure the luminescence emission and decay times of europium in all systems. The excitation wavelength was set at 395 nm because this wavelength allows direct excitation of Eu^{3+} , which avoids the antenna effect of L_2EO_4 . Emission spectra were recorded in the range of 500–750 nm. Excitation spectra were recorded in the range of 250–500 nm.

Analysis of TRL Data. The luminescence intensity I_t can be expressed by eqs 1 and 2 for single- and double-exponential decays, respectively,³⁸

$$I_t = I_1 e^{-t/\tau_1} \quad (1)$$

$$I_t = I_1 e^{-t/\tau_1} + I_2 e^{-t/\tau_2} \quad (2)$$

$$\alpha_i = \frac{I_i}{I_1 + I_2} \quad (3)$$

where I_t is the emission intensity at time t . In the case of single exponential decay, only one decay time can be obtained. If a single luminophore displays two decays, I_i ($i = 1, 2$) is the emission intensity of luminophores in different environments at time 0 and τ_i ($i = 1, 2$) is the decay time of luminescence for luminophores in different environments. In this case, α_i ($i = 1, 2$) values represent the fraction of the luminescence of Eu^{3+} in the i th environment. Because the fraction of Eu^{3+} at the chain end will be decreased when chain extension occurs in the electrostatic micelles, we are able to calculate the average chain length simply from α . Meanwhile, control experiments were carried out in deuterium oxide (D_2O), which does not quench the emission of europium,³⁹ to calculate the number of

water molecules that are still in the coordination sphere by using eq 4²⁸

$$q = 1.2 \times (k_{\text{H}_2\text{O}} + k_{\text{D}_2\text{O}} - 0.25) \quad (4)$$

Here, $k_{\text{H}_2\text{O}}$ and $k_{\text{D}_2\text{O}}$ represent the rate constants of luminescence decay, which are measured in H_2O and D_2O , respectively. The re-evaluated proportionality constant of 1.2 ms signifies the sensitivity of the lanthanide ion to vibronic quenching by the OH oscillators. A correction factor of -0.25 ms^{-1} is applied to allow for the effect of closely diffusing OH oscillators.

As lanthanide ions are known to coordinate with 8–9 water molecules in an aqueous solution,^{40,41} the number of coordinating sites occupied by ligands can be obtained upon subtracting the coordinated water molecules.

The photophysical properties of the Eu^{3+} complexes, including the 4f–4f emission quantum yield (Φ_{in}), the radiative lifetime (τ_{rad}), the radiative constant (k_{r}), and the nonradiative constant (k_{nr}), were estimated from the observed lifetimes (τ_{obs}) and emission spectra using the following equations^{42,43}

$$\Phi_{\text{in}} = \frac{k_{\text{r}}}{k_{\text{r}} + k_{\text{nr}}} = \frac{\tau_{\text{obs}}}{\tau_{\text{rad}}} \quad (5)$$

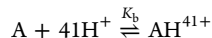
$$\frac{1}{\tau_{\text{rad}}} = A_{\text{MD},0} n^3 \left(\frac{I_{\text{tot}}}{I_{\text{MD}}} \right) \quad (6)$$

$$k_{\text{r}} = \frac{1}{\tau_{\text{rad}}} \quad (7)$$

$$k_{\text{nr}} = \frac{1}{\tau_{\text{obs}}} - \frac{1}{\tau_{\text{rad}}} \quad (8)$$

where $A_{\text{MD},0}$ is the spontaneous emission probability for the $^5\text{D}_0\text{--}^7\text{F}_1$ transition in vacuum (14.65 s^{-1}), n is the refractive index of the medium (an average index of refraction equal to 1.5 was employed), and $(I_{\text{tot}}/I_{\text{MD}})$ is the ratio of the total area of the corrected $\text{Eu}(\text{III})$ emission spectrum to the area of the $^5\text{D}_0\text{--}^7\text{F}_1$ band.

pH Measurements and pH Titration Experiments. pH was measured using a pH meter S40 produced by Mettler-Toledo. The electrode is from InLab Semi-Micro. Before measurements, technical buffer solutions with pH 4.01, 7.00, and 9.21 made by Mettler-Toledo were used to calibrate the pH meter. The degree of quarternization of P2VP₄₁-*b*-PEO₂₀₅ at various pH values was determined using pH titration experiments. A pH titration curve for P2VP₄₁-*b*-PEO₂₀₅ was obtained by recording the variation of solution pH with the volume of added 0.1 M HCl. Then, the $\text{p}K_{\text{b}}$ for P2VP₄₁-*b*-PEO₂₀₅ was obtained. The concentration of protonated P2VP₄₁-*b*-PEO₂₀₅ was calculated based on the following equilibrium



Light-Scattering Measurements. Dynamic light-scattering (DLS) measurements were carried out using a laser light scattering spectrometer ALV/DLS/SLS-5022F of standard design (ALV-5000/E/WIN Multiple Tau Digital Correlator) with a 22 mW He–Ne laser (wavelength: 632.8 nm). The scattering angle was 90°, and the CONTIN method was used to analyze the distribution of the radii of micelles. Nonweighed data were recorded for all experiments.

Transmission Electron Microscopy (TEM). A JEOL 2100F TEM was employed to observe the morphology of micelles. Drops of samples were put onto 230 mesh copper grids coated with a carbon film. Excess water was removed using filter paper, and the samples were then allowed to dry in ambient air at room temperature before TEM observation.

RESULTS AND DISCUSSION

TRL Technique in Probing the Structure of the Free Coordination Complex. Because theoretical calculations have predicted the structure of the free coordination complex in a

Table 1. Summary of Decay Times, Fractions of Long Decay Time Luminophores (α_2), and the Number of Coordinating Water Molecules (q) of the $\text{L}_2\text{EO}_4\text{--Eu}$ Complexes in H_2O (τ_1 , τ_2) and in D_2O (τ)^a

$\text{L}_2\text{EO}_4/\text{Eu}$	H_2O				D_2O		
	τ_1/ms	τ_2/ms	α_2	χ^2	τ/ms	χ^2	q
0/1	0.11		0	1.10	2.38	1.20	8.81
1/1	0.33		0	1.16	2.71	1.18	2.94
3/2	0.59	1.25	0.47	1.17	2.69	1.29	0.21
2/1		1.33	1	1.20	2.59	1.25	0.14
5/2		1.41	1	1.15	2.59	1.16	0.09
3/1		1.43	1	1.26	2.57	1.15	0.07
4/1		1.45	1	1.13	2.57	1.23	0.06
5/1		1.46	1	1.18	2.56	1.25	0.06

^aThe quality of data fitting is expressed as χ^2 ($\lambda_{\text{ex}} = 395 \text{ nm}$, $[\text{Eu}^{3+}] = 0.67 \text{ mM}$, $\text{pH} = 6.9$).

solution,^{17,19} we first studied the structure of the free coordination complex at various metal-to-ligand ratios to evaluate the reliability of the TRL technique in determining the structure of the coordination complex.

Figure 1A shows an increase of UV absorbance with increase in the amount of L_2EO_4 in the Eu^{3+} solution, suggesting stepwise coordination of L_2EO_4 to Eu^{3+} . Meanwhile, the luminescence in Figure 1B also gives a stepwise increase at 593, 613, and 693 nm, which corresponds to the $^5\text{D}_0\text{--}^7\text{F}_1$, $^5\text{D}_0\text{--}^7\text{F}_2$, and $^5\text{D}_0\text{--}^7\text{F}_4$ transitions, respectively. Because the excitation wavelength is set at 395 nm, which excited only the central europium ion rather than the ligand (Figure S1), the luminescence intensity is related only to the water molecules that coordinated with Eu^{3+} ions. Therefore, it is obvious that L_2EO_4 has gradually replaced the water molecules in the first coordination sphere of the coordination of Eu^{3+} .

In Figure 1C, we show the TRL of Eu^{3+} for the $\text{L}_2\text{EO}_4/\text{Eu}$ coordinating complexes at various $\text{L}_2\text{EO}_4/\text{Eu}$ ratios. It is found that the decay rate becomes slower with increase in the ratio (Figure 1C), indicative of increased decay times. The decay times obtained using eqs 1 and 2 are listed in Table 1. It is clear that the decay time reaches a constant value as $\text{L}_2\text{EO}_4/\text{Eu} > 3/1$, suggesting that all nine coordinating sites of one Eu^{3+} ion are occupied by L_2EO_4 at $\text{L}_2\text{EO}_4/\text{Eu} > 3/1$. This is in line with the conclusion obtained with steady-state luminescence (Figure 2B).³¹ The decay times and the number of remaining coordinating water molecules q for the $\text{L}_2\text{EO}_4\text{--Eu}$ systems at all ratios are also given in Table 1. Clearly, q decreases with increasing fraction of L_2EO_4 . Without the addition of L_2EO_4 , the number of water molecules coordinated to a central Eu^{3+} ion is 8.8, which is in good agreement with the literature results, which suggests that 8–9 water molecules can be coordinated to one Eu^{3+} in water.^{40,41}

As indicated in Table 1, only one decay time is obtained for the coordination complexes of the $\text{L}_2\text{EO}_4\text{--Eu}$ system at various ratios except for the $\text{L}_2\text{EO}_4/\text{Eu} = 3/2$ system, suggesting the presence of only one detectable coordinating environment for Eu^{3+} . It is noticed that the q value is about 3 for the $\text{L}_2\text{EO}_4/\text{Eu} = 1/1$ coordination complexes, which implies that six coordination sites of Eu^{3+} are occupied by L_2EO_4 . Because previous studies have shown that the spacer length of L_2EO_4 is not long enough to form an intramolecular complex,¹⁹ this result indicates that a closed ring structure with the composition of $(\text{L}_2\text{EO}_4)_2\text{Eu}_2$ is formed, as has been verified in the $\text{L}_2\text{EO}_4\text{--Zn}$ system.¹⁹ This is rather unexpected for the

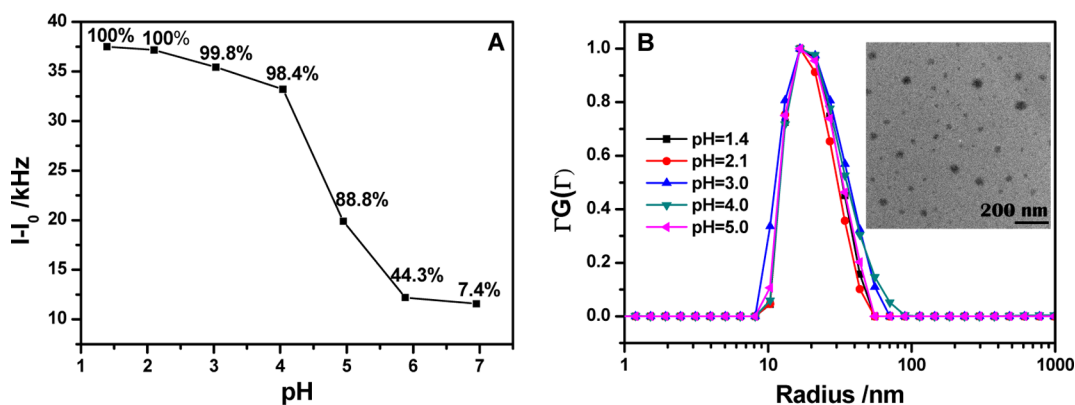
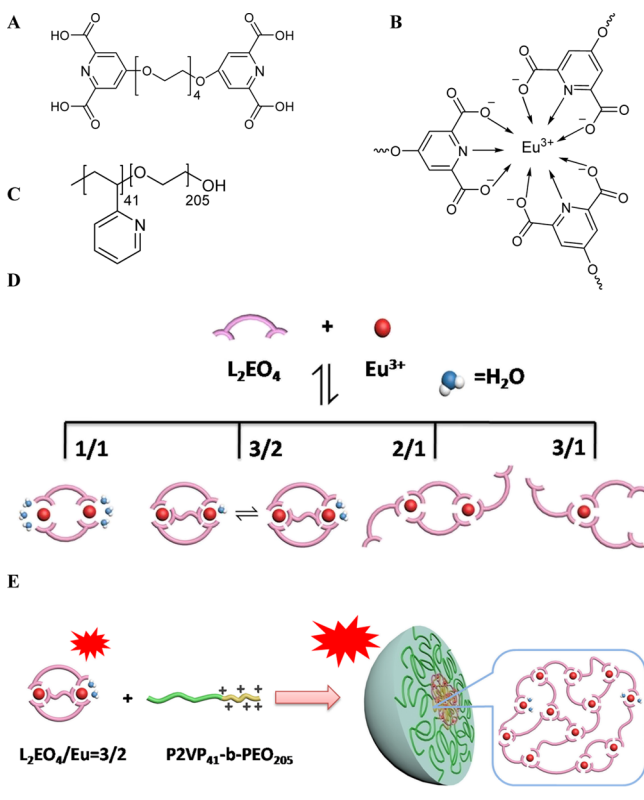


Figure 2. (A) Scattering light intensity of P2VP₄₁-*b*-PEO₂₀₅/L₂EO₄-Eu (3/2) micelles at different pH values (I_0 : scattering light intensity of the solvent); the numbers are the protonation rates of P2VP₄₁-*b*-PEO₂₀₅ at different pH values. $[Eu^{3+}] = 0.67$ mM, and $\lambda_{ex} = 395$ nm. (B) DLS distribution of P2VP₄₁-*b*-PEO₂₀₅/L₂EO₄-Eu (3/2) micelles at different pH values and the TEM image (inset) of the micelles at pH = 4.0.

Scheme 1. (A) Structure of L₂EO₄, (B) Demonstration of the Coordination between the Head of L₂EO₄ and Eu³⁺, (C) Structure of P2VP₄₁-*b*-PEO₂₀₅, (D) Schematic Illustration of the Dominant Coordination Complexes in the L₂EO₄/Eu System at pH 6.9, (E) Illustration of the Chain Extension of the L₂EO₄/Eu = 3/2 System upon Formation of PIC Micelles.



L₂EO₄-Eu³⁺ system because the nine coordinating sites of Eu³⁺ may accommodate three heads from L₂EO₄, which is expected to form branched structures. It is noticed that the decay time for Eu³⁺ ions in water is 0.11 ms, whereas it slightly increases to 0.33 ms in the L₂EO₄/Eu = 1/1 system where six of the nine sites in the coordination sphere are chelated with the ligand. This implies that quenching by water is very significant even in the presence of a small fraction of water, as can be revealed again in the following section.

When the ratio of L₂EO₄/Eu reaches 3/2, two decay times appear, which indicates that the europium ions are in two different coordinating states.¹⁶ These two states can be ascribed to the europium ions that partially and fully coordinated with L₂EO₄, respectively. For Eu³⁺ with long decay times, the q value is about zero, and the fraction for such Eu³⁺ is about 47%. This means that the quantity of Eu³⁺ ions that are partially and fully coordinated with L₂EO₄ is nearly equal. It is worth noting that the short decay time in the 3/2 system increases to 0.59 ms, which is nearly double as that in the 1/1 system, suggesting that the coordinating numbers for the partially coordinated Eu³⁺ are higher than 6. Because each coordinating head may contribute three chelating points, this means that the partially coordinated Eu³⁺ may be in equilibrium between the two structures, as demonstrated in Scheme 1. In line with this, the q value of the partially coordinated Eu³⁺ is 1.3 instead of 3, which probably indicates that the third ligand coordinates to the central Eu³⁺ ion in a more labile way.

As the L₂EO₄/Eu ratio reaches 2/1 or beyond, only one decay time appears. The q value is about zero, which suggests that all nine coordinating sites of Eu³⁺ are occupied by L₂EO₄. It is worth noting that all Eu³⁺ are already fully coordinated with L₂EO₄ at L₂EO₄/Eu = 2/1 instead of 3/1. We infer that the possible structure is as shown in Scheme 1D. However, the decay time in the 2/1 system is shorter than that in the 3/1 system, suggesting that the chance of the quenching by water in the 2/1 system is larger than that in the latter.

Furthermore, the 4f-4f emission quantum yield (Φ_{in}) and the radiative (k_r) and nonradiative (k_{nr}) constants were estimated and are listed in Table 2. By adding L₂EO₄ to the Eu³⁺ solution, k_{nr} reduced from 8.9×10^3 to 3.6×10^3 s⁻¹ and k_r increased from 1.6×10^2 to 3.3×10^2 s⁻¹. The significant reduction in k_{nr} and slight increase in k_r suggest that the main effect of the ligand is replacing coordinated water and reducing the quenching effect.^{42,43}

TRL Technique in Probing the Structure of the Coordination Complex in Micelles. Next, we used the TRL technique to probe the possible structure of coordination complexes in electrostatic micelles. As discussed previously, the L₂EO₄/Eu = 3/2 complex may form well-defined micelles upon addition of an oppositely charged block polyelectrolyte. The block polyelectrolyte used in this work is P2VP₄₁-*b*-PEO₂₀₅, which is positively charged at pH < 6 according to the pH titration experiments (Figure S2). In Figure 2A, we see that strong scattering occurs at pH 1–5, where DLS measurements

Table 2. Photophysical Properties of L_2EO_4 -Eu Complexes in H_2O at Different Molar Ratios^a

L_2EO_4/Eu	τ_{rad}/ms	τ_{obs}/ms	k_r/s^{-1}	k_{nr}/s^{-1}	Φ_{ln}
0/1	6.11	0.11	1.6×10^2	8.9×10^3	0.018
1/1	4.07	0.33	2.4×10^2	2.8×10^3	0.081
3/2	3.19	0.59/1.25	3.1×10^2	$1.4 \times 10^3/4.9 \times 10^2$	0.18/0.39
2/1	3.05	1.33	3.3×10^2	4.2×10^2	0.44
5/2	3.08	1.41	3.2×10^2	3.8×10^2	0.46
3/1	3.06	1.43	3.3×10^2	3.7×10^2	0.47
4/1	2.99	1.45	3.3×10^2	3.6×10^2	0.48
5/1	3.05	1.46	3.3×10^2	3.6×10^2	0.48

^a τ_{rad} and τ_{obs} are the radiative and observed lifetimes, respectively, and k_r and k_{nr} are the radiative and nonradiative constants, respectively; Φ_{ln} is the quantum yield. Experimental conditions: $\lambda_{ex} = 395$ nm, $[Eu^{3+}] = 0.67$ mM, pH = 6.9.

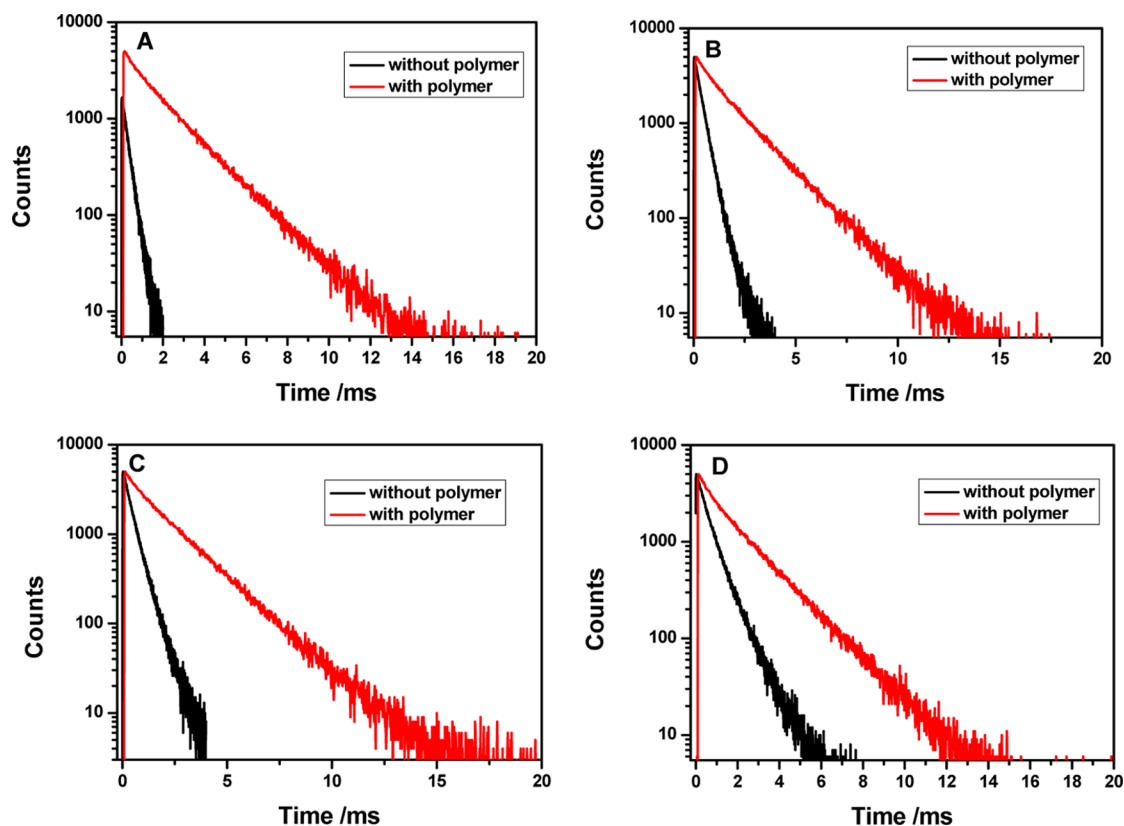


Figure 3. TRL measurement for L_2EO_4 -Eu complexes at 3/2 with and without polymer P2VP₄₁-*b*-PEO₂₀₅: (A) pH = 1.4, (B) pH = 3.0, (C) pH = 4.0, and (D) pH = 4.9 ($[Eu^{3+}] = 0.67$ mM, $\lambda_{ex} = 395$ nm).

Table 3. Summary of Decay Times τ_1 and τ_2 and Fractions of Long Decay Time Fluorophore α_2 of L_2EO_4 -Eu Complexes with and without the Diblock Copolymer at Different pH Values^a

system pH	L_2EO_4 -Eu				L_2EO_4 -Eu/P2VP ₄₁ - <i>b</i> -PEO ₂₀₅			
	τ_1/ms	τ_2/ms	χ^2	α_2	τ_1/ms	τ_2/ms	χ^2	α_2
1.4	0.28		1.19	0	0.68	1.98	1.10	0.80
2.1	0.35		1.20	0	0.68	1.99	1.15	0.79
3.0	0.37		1.19	0	0.54	1.95	1.14	0.79
4.0	0.35	0.62	1.20	0.32	0.46	1.98	1.20	0.83
4.9	0.45	0.91	1.16	0.36	0.49	1.93	1.16	0.74

^aThe quality of data fitting is expressed as χ^2 ($\lambda_{ex} = 395$ nm, $[Eu^{3+}] = 0.67$ mM, $L_2EO_4/Eu = 3/2$).

revealed the presence of particles with an average radius of 18 nm. This is consistent with the size of micelles formed in our

previous observations and again confirmed using TEM observation in Figure 2B,^{20,25} suggesting that micelles are indeed formed in these systems. It is remarkable that the scattering intensity increases as pH decreases (Figure 2B), suggesting that more micelles are formed at acidic pH. This is because the diblock polymer carries more positive charges under acidic conditions owing to the protonation of the pyridine groups, which facilitates the electrostatic interaction with the negatively charged L_2EO_4/Eu complexes.

In Table 2 and Figure 3, we show the TRL results of the $L_2EO_4/Eu = 3/2$ system at various pH values with and without the presence of the block copolymer. It is remarkable that without the presence of the polymer, the $L_2EO_4/Eu = 3/2$ system at pH < 4 forms only a short-life coordinating complex, which indicates that all Eu^{3+} ions are partially coordinated. This is because both the N atom and the COO^- groups in the L_2EO_4 molecule are protonated at acidic pH, so that the ligand cannot form an effective coordination bond with Eu^{3+} ions. As

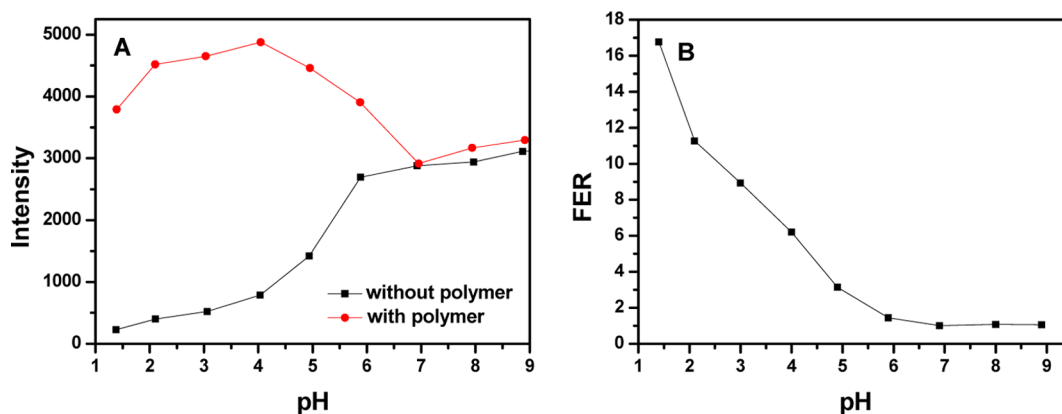


Figure 4. (A) The emission intensity at 614 nm of the $L_2EO_4/Eu = 3/2$ system with and without diblock copolymer P2VP₄₁-*b*-PEO₂₀₅ at different pH values. (B) The luminescence enhancement ratios at different pH values (FER, defined as the ratio of intensities in the presence and in the absence of the diblock copolymer) at $L_2EO_4/Eu = 3/2$ ($[Eu^{3+}] = 0.67$ mM, $\lambda_{ex} = 395$ nm).

Table 4. Photophysical Properties of $L_2EO_4/Eu = 3/2$ Complexes in H_2O at Different pH Values^a

pH	τ_{rad}/ms	τ_{obs}/ms	k_r/s^{-1}	k_{nr}/s^{-1}	Φ_{in}
1.4	4.08	0.28	2.4×10^2	3.3×10^3	0.068
2.1	3.87	0.35	2.6×10^2	2.6×10^3	0.090
3.0	3.94	0.37	2.5×10^2	2.4×10^3	0.094
4.0	3.58	0.35/0.62	2.8×10^2	$2.4 \times 10^3/1.3 \times 10^3$	0.098/0.17
4.9	3.20	0.45/0.91	3.1×10^2	$1.9 \times 10^3/7.8 \times 10^2$	0.14/0.28

^a τ_{rad} and τ_{obs} are the radiative and observed lifetimes, respectively, and k_r and k_{nr} are the radiative and nonradiative constants, respectively; Φ_{in} is the quantum yield ($\lambda_{ex} = 395$ nm, $[Eu^{3+}] = 0.67$ mM).

Table 5. Photophysical Properties of L_2EO_4/Eu Complexes with the Diblock Copolymer at Different pH Values^a

pH	τ_{rad}/ms	τ_{obs}/ms	k_r/s^{-1}	k_{nr}/s^{-1}	Φ_{in}
1.4	3.61	0.68/1.98	2.8×10^2	$1.2 \times 10^3/2.3 \times 10^2$	0.19/0.55
2.1	3.53	0.68/1.99	2.8×10^2	$1.2 \times 10^3/2.2 \times 10^2$	0.19/0.56
3.0	3.53	0.54/1.95	2.8×10^2	$1.6 \times 10^3/2.3 \times 10^2$	0.15/0.55
4.0	3.44	0.46/1.98	2.9×10^2	$1.9 \times 10^3/2.1 \times 10^3$	0.13/0.58
4.9	3.45	0.49/1.93	2.9×10^2	$1.8 \times 10^3/2.3 \times 10^2$	0.14/0.56

^a τ_{rad} and τ_{obs} are the radiative and observed lifetimes, respectively, and k_r and k_{nr} are the radiative and nonradiative constants, respectively; Φ_{in} is the quantum yield ($\lambda_{ex} = 395$ nm, $L_2EO_4/Eu = 3/2$, $[Eu^{3+}] = 0.67$ mM).

pH increases, the coordinating ability of L_2EO_4 increases as well. It is remarkable that upon addition of the block copolymer into these systems, the decay time increases to about 2 ms in all solutions. Control experiments suggest that the number of coordinating water molecules q in these states is zero (obtained using the parameters $\tau_{D_2O} = 2.95$ ms and $\tau_{micelle} = 2.95$ ms). This implies that in the micelles, all of the coordinating sites of the Eu^{3+} ion are taken by L_2EO_4 . According to eq 3, the fraction of long decay time Eu^{3+} amounts to the maximum value of 83% at pH 4 (Table 3), suggesting that at this pH the degree of "polymerization" for the L_2EO_4 -Eu coordinating system is the largest. This is in line with the observation of the maximum luminescence intensity at the same pH (Figure 4A). The long decay time is contributed by the europium ions that are fully coordinated with L_2EO_4 , verifying that the chain extension for the L_2EO_4/Eu coordinating complex indeed occurs in the micellar core. It is remarkable that even under the very acidic conditions of pH 1–3, the fraction for Eu^{3+} ions fully coordinated with L_2EO_4 is about 80% in the micelles, whereas that for the free coordination complexes under the same conditions is zero. Meanwhile, the emission intensity is enhanced by a factor of 9 and 16 for systems at pH 3.0 and 1.4 (Figures 4B, S3, and S4), respectively, suggesting that

micellization facilitates coordination between L_2EO_4 and Eu^{3+} . This indicates that the formation of micelles and coordination supramolecular polymer occurs synergistically. It can be inferred from the TRL results that in the presence of oppositely charged block copolymers, L_2EO_4 prefers coordination with Eu^{3+} instead of protonation.

Table 3 tells that the number of coordinating water molecules q of partially coordinated Eu^{3+} in the micellar system at pH = 4 is 1.9 (≈ 2) instead of 3. Each head of L_2EO_4 contributes three chelating points, indicating that three heads have participated in chelation, but probably the third head chelated to the Eu^{3+} with only one site, as illustrated in Scheme 1E, because of steric hindrance. Most importantly, the TRL results indicate that on average, there were no Eu^{3+} ions chelating 6 or 3 water molecules, suggesting that there are no coordinating ends in the micellar core. In other words, the Eu^{3+} and L_2EO_4 exist in the micellar core in the form of one whole network. This is the first qualitative analysis for the extent of chain extension enhanced by electrostatic micellization, which we were not able to know before this study.

Also, we calculated Φ_{in} , k_r , and k_{nr} of $L_2EO_4/Eu = 3/2$ complexes with and without the diblock copolymer and listed the data in Tables 4 and 5. As expected, the k_{nr} of $L_2EO_4/Eu =$

3/2 complexes is large because of the protonation of ligands, which weakens the coordination effect. By adding the diblock polymer, k_{nr} was reduced significantly. The k_r values of the $L_2EO_4/Eu = 3/2$ complex with and without the polymer under different conditions are almost the same, which suggests that this value probably depends on the properties of ligands. These results confirm that the main effect of ligands is reducing the quenching by water molecules.

CONCLUSIONS

In conclusion, we have employed the TRL technique to probe the in situ structure of reversible coordination polymers in their electrostatic micelles. Upon analyzing the luminescence intensity decay rate, we obtained the coordination information of the europium ions, which directly correlates with the structure of the coordinating system. In this way, we are able to know the polymerization degree of the coordinating complex. We expect that the method established in this work may provide fundamental information on the structure change in reversible coordination polymer systems and may help to explain, understand, and predict relevant properties and functions.

ASSOCIATED CONTENT

Supporting Information

The Supporting Information is available free of charge on the ACS Publications website at DOI: 10.1021/acs.langmuir.6b00967.

Additional experimental results for the excitation spectra of the L_2EO_4 -Eu complex, pH titration, the emission spectra for the L_2EO_4 -Eu complexes at various pH values, the emission spectra of L_2EO_4 -Eu/P2VP₄₁-PEO₂₀₅ at fixed pH, and the comparison between these two groups Figures S1–S5; the summary of evolutions of the transitions of L_2EO_4 -Eu complexes in H₂O at different molar ratios and the summary of evolutions of the transitions of L_2EO_4 -Eu complexes with and without the polymer in H₂O at different pH values Tables S1 and S2 (PDF)

AUTHOR INFORMATION

Corresponding Authors

*E-mail: jbhuan@pku.edu.cn (J.H.).

*E-mail: yunyan@pku.edu.cn (Y.Y.).

Notes

The authors declare no competing financial interest.

ACKNOWLEDGMENTS

The authors acknowledge financial support from the National Natural Science Foundation of China (Grant No. 21422302, 21573011, and 21473005) and the Beijing National Laboratory for Molecular Sciences (BNLMS).

REFERENCES

- (1) Friese, V. A.; Kurth, D. G. Soluble dynamic coordination polymers as a paradigm for materials science. *Coord. Chem. Rev.* **2008**, *252*, 199–211.
- (2) Yan, Y.; Huang, J. Hierarchical assemblies of coordination supramolecules. *Coord. Chem. Rev.* **2010**, *254*, 1072–1080.
- (3) Yang, W.-Q.; Liu, H.-G.; Liu, G.-K.; Lin, Y.; Gao, M.; Zhao, X.-Y.; Zheng, W.-C.; Chen, Y.; Xu, J.; Li, L.-Z. Trivalent europium-doped strontium molybdate red phosphors in white light-emitting diodes:

Synthesis, photophysical properties and theoretical calculations. *Acta Mater.* **2012**, *60*, 5399–5407.

- (4) Jung, J. H.; Lee, J. H.; Silverman, J. R.; John, G. Coordination polymer gels with important environmental and biological applications. *Chem. Soc. Rev.* **2013**, *42*, 924–936.

- (5) Beck, J. B.; Rowan, S. J. Multistimuli, multiresponsive metallo-supramolecular polymers. *J. Am. Chem. Soc.* **2003**, *125*, 13922–13923.

- (6) Weng, W.; Li, Z.; Jamieson, A. M.; Rowan, S. J. Control of Gel Morphology and Properties of a Class of Metallo-Supramolecular Polymers by Good/Poor Solvent Environments. *Macromolecules* **2009**, *42*, 236–246.

- (7) Burnworth, M.; Tang, L.; Kumpfer, J. R.; Duncan, A. J.; Beyer, F. L.; Fiore, G. L.; Rowan, S. J.; Weder, C. Optically healable supramolecular polymers. *Nature* **2011**, *472*, 334–337.

- (8) Miller, A. K.; Li, Z.; Streletsky, K. A.; Jamieson, A. M.; Rowan, S. J. Redox-induced polymerisation/depolymerisation of metallo-supramolecular polymers. *Polym. Chem.* **2012**, *3*, 3132.

- (9) Khlobystov, A. N.; Blake, A. J.; Champness, N. R.; Lemenovskii, D. A.; Majouga, A. G.; Zyk, N. V.; Schroder, M. Supramolecular design of one-dimensional coordination polymers based on silver(I) complexes of aromatic nitrogen-donor ligands. *Coord. Chem. Rev.* **2001**, *222*, 155–192.

- (10) Paulusse, J. M. J.; van Beek, D. J. M.; Sijbesma, R. P. Reversible switching of the sol–gel transition with ultrasound in rhodium(I) and iridium(I) coordination networks. *J. Am. Chem. Soc.* **2007**, *129*, 2392–2397.

- (11) Schütte, M.; Kurth, D. G.; Linford, M. R.; Cölfen, H.; Möhwald, H. Metallo-supramolecular thin polyelectrolyte films. *Angew. Chem., Int. Ed.* **1998**, *37*, 2891–2893.

- (12) Kurth, D. G.; Schütte, M.; Wen, J. Metallo-supramolecular polyelectrolyte multilayers with cobalt(II): preparation and properties. *Colloids Surf., A* **2002**, *198*, 633–643.

- (13) Caruso, F.; Schüler, C.; Kurth, D. G. Core–shell particles and hollow shells containing metallo-supramolecular components. *Chem. Mater.* **1999**, *11*, 3394–3399.

- (14) Meister, A.; Förster, G.; Thünemann, A. F.; Kurth, D. G. Nanoscopic structure of a metallo-supramolecular polyelectrolyte-amphiphile complex, elucidated by X-ray scattering and molecular modeling. *ChemPhysChem* **2003**, *4*, 1095–1100.

- (15) Kurth, D. G.; Severin, N.; Rabe, J. P. Perfectly straight nanostructures of metallosupramolecular coordination-polyelectrolyte amphiphile complexes on graphite. *Angew. Chem., Int. Ed.* **2002**, *41*, 3681–3683.

- (16) Schwarz, G.; Bodenthin, Y.; Tomkowicz, Z.; Haase, W.; Geue, T.; Kohlbrecher, J.; Pietsch, U.; Kurth, D. G. Tuning the Structure and the Magnetic Properties of Metallo-supramolecular Polyelectrolyte–Amphiphile Complexes. *J. Am. Chem. Soc.* **2011**, *133*, 547–558.

- (17) Chen, C.-C.; Dormidontova, E. E. Supramolecular polymer formation by metal–ligand complexation: Monte Carlo simulations and analytical modeling. *J. Am. Chem. Soc.* **2004**, *126*, 14972–14978.

- (18) Kurth, D. G.; Lehmann, P.; Schütte, M. A route to hierarchical materials based on complexes of metallosupramolecular polyelectrolytes and amphiphiles. *Proc. Natl. Acad. Sci. U.S.A.* **2000**, *97*, 5704–5707.

- (19) Vermonden, T.; van der Gucht, J.; de Waard, P.; Marcelis, A. T. M.; Besseling, N. A. M.; Sudhölter, E. J. R.; Fleer, G. J.; Stuart, M. A. C. Water-soluble reversible coordination polymers: Chains and rings. *Macromolecules* **2003**, *36*, 7035–7044.

- (20) Yan, Y.; Besseling, N. A. M.; de Keizer, A.; Marcelis, A. T. M.; Drechsler, M.; Cohen Stuart, M. A. Hierarchical Self-Assembly in Solutions Containing Metal Ions, Ligand, and Diblock Copolymer. *Angew. Chem., Int. Ed.* **2007**, *46*, 1807–1809.

- (21) Yan, Y.; Martens, A. A.; Besseling, N. A. M.; de Wolf, F. A.; de Keizer, A.; Drechsler, M.; Cohen Stuart, M. A. Nanoribbons self-assembled from triblock peptide polymers and coordination polymers. *Angew. Chem., Int. Ed.* **2008**, *47*, 4192–4195.

- (22) Wang, J.; de Keizer, A.; Fokkink, R.; Yan, Y.; Cohen Stuart, M. A.; van der Gucht, J. Complex Coacervate Core Micelles from Iron-

Based Coordination Polymers. *J. Phys. Chem. B* **2010**, *114*, 8313–8319.

(23) Wang, J.; de Keizer, A.; van Leeuwen, H. P.; Yan, Y.; Vergeldt, F.; van As, H.; Bomans, P. H. H.; Sommerdijk, N. A. J. M.; Cohen Stuart, M. A.; van der Gucht, J. Effect of pH on Complex Coacervate Core Micelles from Fe(III)-Based Coordination Polymer. *Langmuir* **2011**, *27*, 14776–14782.

(24) Wang, J.; Velders, A. H.; Gianolio, E.; Aime, S.; Vergeldt, F. J.; Van As, H.; Yan, Y.; Drechsler, M.; de Keizer, A.; Cohen Stuart, M. A.; van der Gucht, J. Controlled mixing of lanthanide(III) ions in coacervate core micelles. *Chem. Commun.* **2013**, *49*, 3736–3738.

(25) Yang, L.; Ding, Y.; Yang, Y.; Yan, Y.; Huang, J.; de Keizer, A.; Cohen Stuart, M. A. Fluorescence enhancement by microphase separation-induced chain extension of Eu³⁺ coordination polymers: phenomenon and analysis. *Soft Matter* **2011**, *7*, 2720.

(26) Lan, Y.; Xu, L.; Yan, Y.; Huang, J.; de Keizer, A.; Besseling, N. A. M.; Cohen Stuart, M. A. Promoted formation of coordination polyelectrolytes by layer-by-layer assembly. *Soft Matter* **2011**, *7*, 3565.

(27) Liang, Y.; Xu, L.; Zhou, Y.; Zhang, X.; Huang, J.; Yan, Y. Decreasing operating potential for water electrolysis to hydrogen via local confinement of iron-based soft coordination suprapolymers. *Phys. Chem. Chem. Phys.* **2013**, *15*, 15912–15916.

(28) Beeby, A.; Clarkson, I. M.; Dickins, R. S.; Faulkner, S.; Parker, D.; Royle, L.; de Sousa, A. S.; Williams, J. A. G.; Woods, M. Non-radiative deactivation of the excited states of europium, terbium and ytterbium complexes by proximate energy-matched OH, NH and CH oscillators: an improved luminescence method for establishing solution hydration states. *J. Chem. Soc., Perkin Trans. 2* **1999**, 493–504.

(29) Bünzli, J.-C. G.; Pigué, C. Taking advantage of luminescent lanthanide ions. *Chem. Soc. Rev.* **2005**, *34*, 1048.

(30) Supkowski, R. M.; Horrocks, W. D. On the determination of the number of water molecules, *q*, coordinated to europium(III) ions in solution from luminescence decay lifetimes. *Inorg. Chim. Acta* **2002**, *340*, 44–48.

(31) Xu, L.; Jing, Y.; Feng, L.; Xian, Z.; Yan, Y.; Liu, Z.; Huang, J. The advantage of reversible coordination polymers in producing visible light sensitized Eu(III) emissions over EDTA via excluding water from the coordination sphere. *Phys. Chem. Chem. Phys.* **2013**, *15*, 16641–16647.

(32) Zhang, R.-J.; Liu, H.-G.; Yang, K. Z.; Si, Z.-K.; Zhu, G.-Y.; Zhang, H.-W. Fabrication and fluorescence characterization of the LB films of luminous rare earth complexes Eu(TTA)₃ Phen and Sm(TTA)₃ Phen. *Thin Solid Films* **1997**, *295*, 228–233.

(33) Zhang, R.; Lu, D.; Lin, Z.; Li, L.; Jin, W.; Möhwal, H. Enriched encapsulation and fluorescence enhancement of europium complexes in microcapsules. *J. Mater. Chem.* **2009**, *19*, 1458.

(34) Wang, C.; Zhang, R.; Möhwal, H. Micelles as “Fluorescence Protector” for an Europium Complex in Microcapsules. *Langmuir* **2010**, *26*, 11987–11990.

(35) Yang, C.; Fu, L.-M.; Wang, Y.; Zhang, J.-P.; Wong, W.-T.; Ai, X.-C.; Qiao, Y.-F.; Zou, B.-S.; Gui, L.-L. A highly luminescent europium complex showing visible-light-sensitized red emission: Direct observation of the singlet pathway. *Angew. Chem., Int. Ed.* **2004**, *43*, 5010–5013.

(36) Law, G.-L.; Pham, T. A.; Xu, J.; Raymond, K. N. A Single Sensitizer for the Excitation of Visible and NIR Lanthanide Emitters in Water with High Quantum Yields. *Angew. Chem., Int. Ed.* **2012**, *51*, 2371–2374.

(37) Vermond, T.; de Vos, W. M.; Marcelis, A. T. M.; Sudhölter, E. J. R. 3-D water-soluble reversible neodymium(III) and lanthanum(III) coordination polymers. *Eur. J. Inorg. Chem.* **2004**, 2847–2852.

(38) Lakowicz, J. R. *Principles of Fluorescence Spectroscopy*; Springer: Berlin, 2006; pp 141–142.

(39) Bünzli, J.-C. G. Lanthanide Luminescence for Biomedical Analyses and Imaging. *Chem. Rev.* **2010**, *110*, 2729–2755.

(40) Horrocks, W. D.; Sudnick, D. R. Lanthanide ion probes of structure in biology. Laser-induced luminescence decay constants provide a direct measure of the number of metal-coordinated water molecules. *J. Am. Chem. Soc.* **1979**, *101*, 334–340.

(41) Marmodée, B.; Jahn, K.; Ariese, F.; Gooijer, C.; Kumke, M. U. Direct Spectroscopic Evidence of 8- and 9-fold Coordinated Europium(III) Species in H₂O and D₂O. *J. Phys. Chem. A* **2010**, *114*, 13050–13054.

(42) Moreau, P.; Colette-Maatouk, S.; Vitorge, P.; Gareil, P.; Reiller, P. E. Complexation of europium(III) by hydroxybenzoic acids: A time-resolved luminescence spectroscopy study. *Inorg. Chim. Acta* **2015**, *432*, 81–88.

(43) Marmodée, B.; de Klerk, J.; Kumke, M. U.; Ariese, F.; Gooijer, C. Spectroscopic investigations of complexes between Eu(III) and aromatic carboxylic ligands. *J. Alloys Compd.* **2008**, *451*, 361–364.